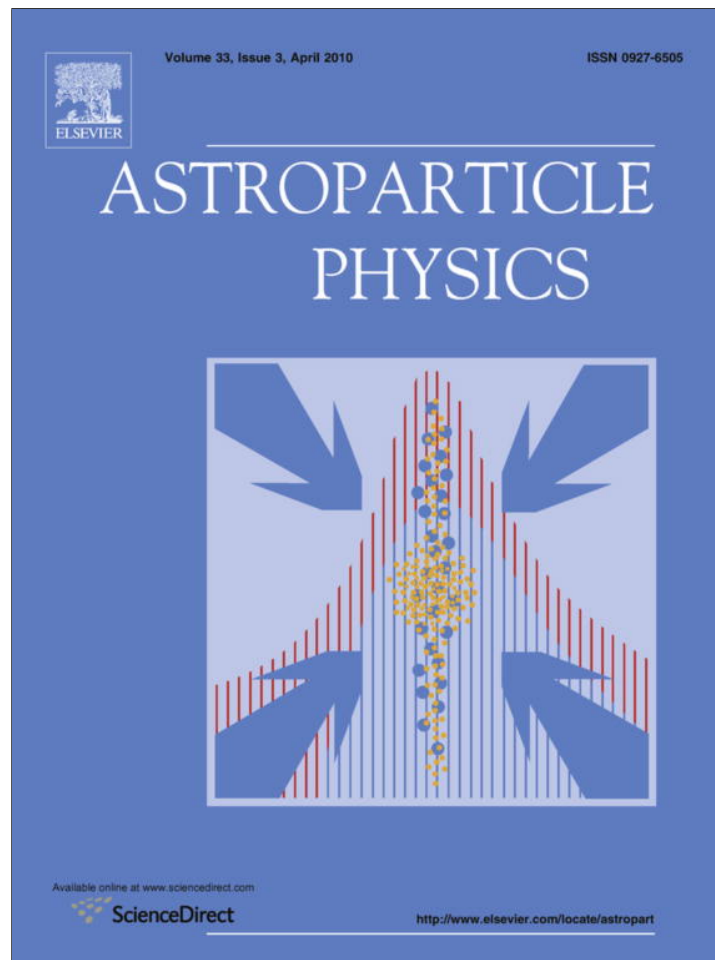


Provided for non-commercial research and education use.
Not for reproduction, distribution or commercial use.



This article appeared in a journal published by Elsevier. The attached copy is furnished to the author for internal non-commercial research and education use, including for instruction at the authors institution and sharing with colleagues.

Other uses, including reproduction and distribution, or selling or licensing copies, or posting to personal, institutional or third party websites are prohibited.

In most cases authors are permitted to post their version of the article (e.g. in Word or Tex form) to their personal website or institutional repository. Authors requiring further information regarding Elsevier's archiving and manuscript policies are encouraged to visit:

<http://www.elsevier.com/copyright>



Contents lists available at ScienceDirect

Astroparticle Physics

journal homepage: www.elsevier.com/locate/astropart

Investigation of cosmic ray anisotropy based on Tsumeb neutron monitor data

G.G. Karapetyan

Cosmic Ray Division, Yerevan Physics Institute, Yerevan 0036, Armenia

ARTICLE INFO

Article history:

Received 26 June 2009

Received in revised form 22 December 2009

Accepted 4 January 2010

Available online 7 January 2010

Keywords:

Sidereal variations

Cosmic rays anisotropy

Asymptotic direction

Heliotail

ABSTRACT

We investigate sidereal daily variations of galactic cosmic rays (CR) by using Tsumeb neutron monitor's (NM) hourly count during 1977–2000. For that purpose a special data analysis is applied to remove solar induced daily variations and improve sidereal variations. Then, the declination of protons in the Earth's magnetosphere is analyzed for the proper determination of particles' asymptotic directions. As a result we found $\sim 0.07\%$ anisotropy with an excess flux from the direction of the right ascension (RA) ~ 6 h. The reversal of solar magnetic field from the negative polarity state (in the time interval 1977–1989) to the positive state (in the interval 1990–2000) does not decrease the amplitude of anisotropy, which means that the origin of anisotropy found is “heliospheric” and not “galactic”. We conclude that the observed anisotropy is a *tail-in anisotropy*, which has been discovered earlier for higher energy (150 GeV–10 TeV) particles in several experiments with underground muon monitors and air-shower detectors. It is believed that the tail-in anisotropy is caused by heliotail boundary, located in the direction RA ~ 6 h, where the interaction between galactic and solar magnetic fields produces CR acceleration

© 2010 Elsevier B.V. All rights reserved.

1. Introduction

Sidereal variations of galactic cosmic rays (CR) flux in energy range 150 GeV–10 TeV had been investigated for many years [1–12] by using both underground muon telescopes and ground based air-shower facilities data. One of the key discoveries was the flux, reaching the maximum at the local sidereal time (LST) ~ 6 h. Analyzing the shapes of the sidereal daily variations, Nagashima et al. [11,12] proposed that there are two anisotropic distributions of particles with energy up to 10 TeV in heliosphere. One is the galactic anisotropy exhibiting a deficit flux from direction RA ~ 0 h. The other is so called *tail-in anisotropy*, characterized by an excess flux, coming from the direction of heliotail RA ~ 6 h. The obtained results deny the existence of anisotropy known as Compton-getting effect [13]. This anisotropy would have been caused due to rotation of solar system around the Galactic center. It was believed that the relative motion between the solar system and surrounding CR plasma would lead to an excess flux, coming from the direction of the motion RA ~ 18 h. However, the absence of an excess flux implies that the heliosphere drags the surrounding CR plasma with it.

At present two anisotropy directions for energy range (150 GeV–10 TeV) are determined: tail-in and loss-cone anisotropies. It is believed that the tail-in anisotropy is caused by heliotail, where the interaction between the galactic and solar magnetic fields induces an additional increase in CR flux. Annual variations in anisotropy amplitude, investigated in Refs. [12,14], showed lar-

ger amplitude of tail-in anisotropy in winter solstice. The authors connect this effect to the closer position of the Earth to the heliotail in winter.

Apart from these studies, a number of investigations have been done with lower energy particle detectors, including: muon telescopes and ion chambers in energy range 60–100 GeV [15], as well as neutron monitors in the range of < 20 GeV [16,17]. In the first case of 60–100 GeV particles, both types of anisotropy have been observed: loss-cone, with a deficit flux coming from the direction RA = 12 h and tail-in, with an excess flux, coming from the direction RA = 6 h. In the case of < 20 GeV particles, loss-cone anisotropy was not observed, and apart from the tail-in anisotropy, another excess of flux from the direction RA = 18 h is reported in [17]. Note, that the existence of tail-in and the absence of loss-cone anisotropy are reported also in another experiment with ~ 60 GeV particles [18].

In all these studies an assumption is made that the asymptotic directions of particles, normally falling on the detector are close to zenith direction. While for > 150 GeV particles this assumption is approximately true, for lower energy particles it is invalid. The reason is that the lower energy particles significantly deflect in the Earth's magnetosphere, causing their asymptotic direction to differ from the zenith direction. For example asymptotic direction of 25 GeV protons, vertically falling on Tsumeb NM differs from Tsumeb zenith direction at the angle $\sim 43^\circ$. In Refs. [16,17] this fact is not taken into account.

In the present paper we investigate sidereal anisotropy on the base of Tsumeb NM data during 1977–2000 by deriving and using a median angle between asymptotic and zenith directions.

E-mail address: grigori@mail.yerphi.am

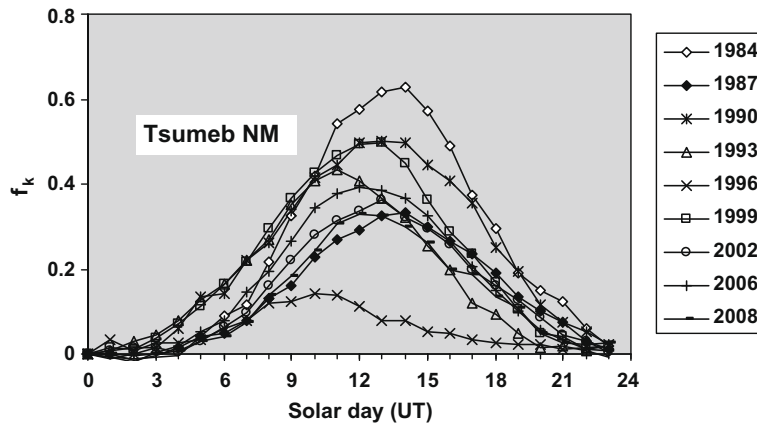


Fig. 1. Solar daily variations of Tsumeb NM in 1984–2008. Maximal count is observed close to the middle of the day.

The structure of the paper is the following. In Section 2 the method of removing solar variations in NM count to reduce noisy signal is described, in Section 3 median energy and angle between the asymptotic and zenith directions for Tsumeb NM are derived, in Section 4 the results are discussed and conclusions are formed.

2. Data analysis

We have used the pressure corrected hourly count of Tsumeb NM. The count changes occasionally by a few percents during a year due to solar activity. Such drift introduces random fluctuations, which deteriorate sidereal variations. To reduce this drift we apply a special procedure as described below.

Let us define NM hourly count as N_j , where $j=0, 1, \dots, 364 \cdot 24$ (for leap-years $365 \cdot 24$).

First a daily (24 h) averaged count d_i is determined for each day according to the formula

$$d_i = \frac{1}{24} \sum_{j=24i}^{24i+23} N_j \quad i = 0, 1, \dots, 364 \quad (1)$$

In [6] the very function d_i is extracted from each hourly record to compensate solar induced variations. For high energy (>160 GeV) particles as in [6], solar induced drift is small, so extracting d_i is quiet sufficient for improving the data. However, in our case of NM count, which is created by lower energy CR, the solar induced occasional drift is large, thus more effective procedure is required. For this we use daily solar variations f_k by the formula

$$g_k = \sum_{i=0}^{364} N_{k+24i}, \quad f_k = 100 \left(\frac{g_k}{g_0} - 1 \right) \quad k = 0, 1, \dots, 23 \quad (2)$$

The function f_k shows averaged variation of NM count during a solar day of 24 h. It reaches the maximum close to the middle of the day as it is seen in Fig. 1.

We should extract this function, multiplied by the corresponding value of the daily averaged count d_i from the hourly count N_j . To do this, let us compose a periodic function F_j ($j=0, 1, \dots, 364 \cdot 24$) with a period of 24 h (i.e. $F_j = F_{j+24}$). Function F_j in the interval $j = 0, \dots, 23$, matches function g_k . Let us also define a function G_j so that

$$G_j = d_i \frac{F_j}{F_0} \quad (3)$$

$$24i \leq j \leq 24i + 23 \quad (4)$$

Here, in order to calculate G_j , one should first take successively $i = 0, 1, \dots, 363$, and for each i to determine the values of j according to (4). Then function G_j is calculated by (3).

By extracting G_j we come to an improved hourly count $M_j = N_j - G_j + N_0$, where the solar induced occasional drift is effectively removed. Functions d_j , G_j as well as raw N_j and improved

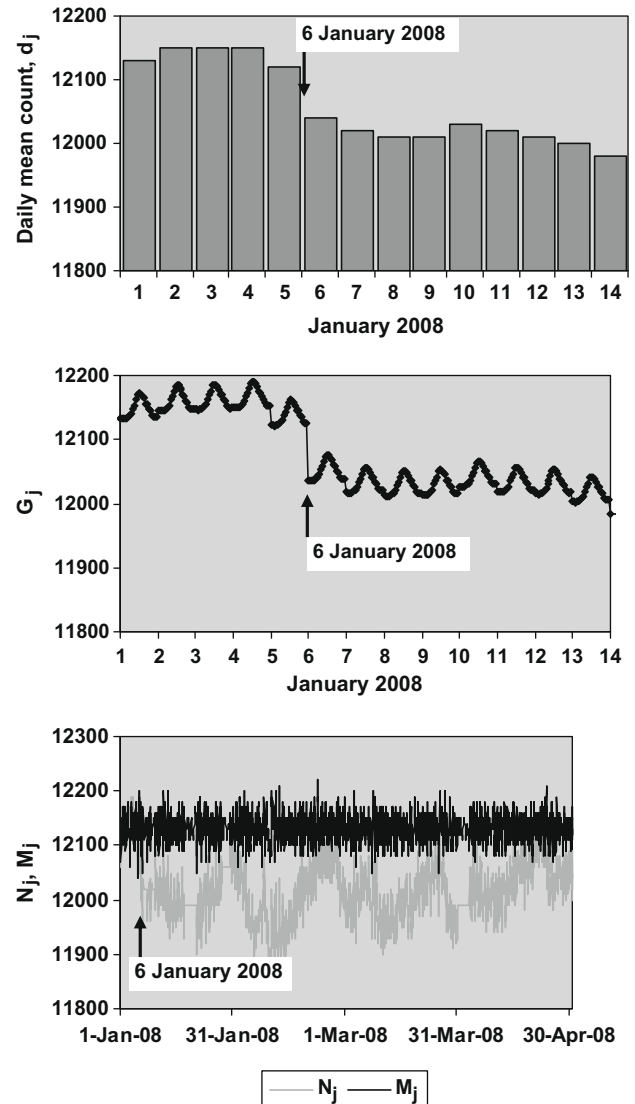


Fig. 2. Functions d_j , G_j , as well as raw and improved counts N_j , M_j . The arrows show a sharp change in raw count N_j at 6 January 2008. It leads to appropriate changes in d_j and G_j , so that the resulting count M_j is significantly improved.

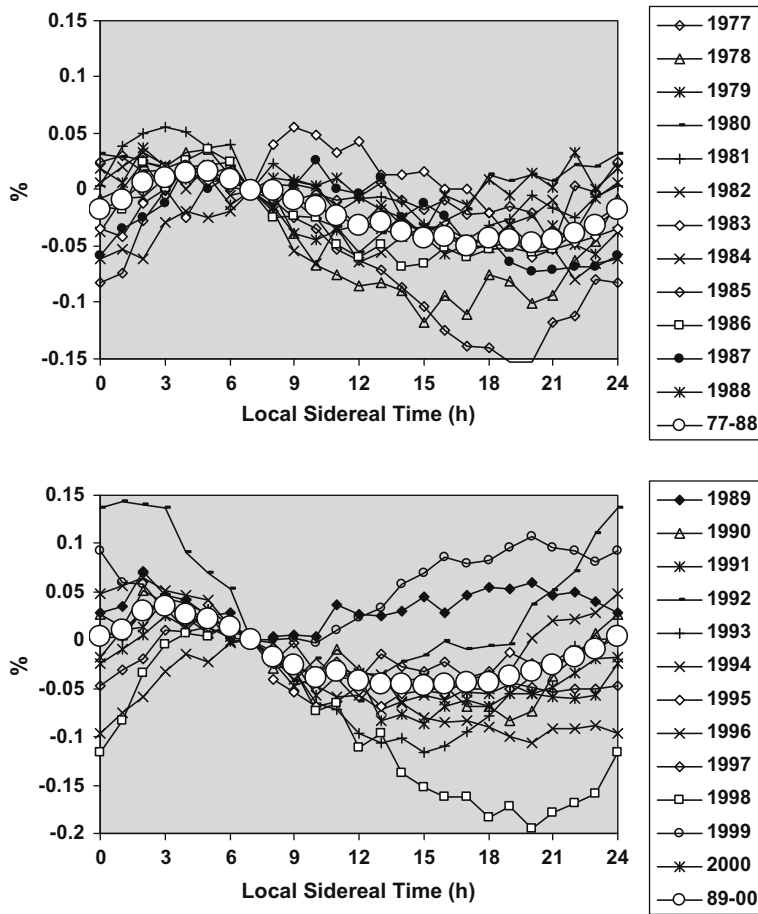


Fig. 3. Sidereal variations of Tsumeb NM count in percentages during the periods 1977–1988 and 1989–2000.

M_j counts are shown in Fig. 2. Note that our used procedure improves also possible biasing of the data in years of solar maximum, caused by Forbush decreases. We see in Fig. 2 that functions d_j and G_j repeat any sharp changes in the raw count N_j (e.g. at 6 January 2008), so that resulting count M_j is significantly improved. Using the improved count M_j we finally derive sidereal hourly variations by binning each hourly count M_j according to its sidereal hour. As a result sidereal variations are obtained, having maximal amplitude $\sim 0.05\text{--}0.07\%$ near $LST \sim 3$ h (see Fig. 3). Now we should determine asymptotic direction, corresponding to observed sidereal times, i.e. to convert x-axis in Fig. 3 to the particle asymptotic directions in units of RA. Since particles suffer magnetic deflection in the Earth's magnetosphere, their falling and asymptotic directions do not coincide.

3. Flux of primaries versus asymptotic direction

Consider particles, which normally fall on NM. They are created by primary particles normally falling on the top of atmosphere, i.e. falling direction of these particles matches zenith direction. However, the asymptotic direction differs from the zenith direction due to the deflection of particles in the Earth's magnetosphere. The bigger is the rigidity of primary particle, the closer its asymptotic direction is to the zenith. On the other hand the bigger the rigidity of primary particle, the smaller flux of such particles, according to the power low spectrum of CR. Therefore, in order to determine the dependence of NM count on the asymptotic direction of primary particles, one needs to convolve the relationships of (i) NM count versus the rigidity of primaries and (ii) asymptotic direction versus the rigidity of primaries.

NM count versus the rigidity is given by Dorman's coupling function $W(R)$, presented in [19]. The function $W(R) = 0$ if $R < R_c$, otherwise it is written as the following (note that the equation for $W(R)$ in [19] has printed incorrectly, so one should use below presented correct Eq. (5))

$$W(R) = \frac{ak}{1 - \exp\left(-\frac{a}{R_c^k}\right)} \frac{1}{R^{k+1}} \exp\left(-\frac{a}{R^k}\right), \quad (5)$$

$$a = (-2.91h^2 - 2.23h - 8.65) \ln(I_{CL}/100) + 24.6h^2 + 19.5h + 81.2$$

$$k = (0.18h^2 - 0.849h + 0.75) \ln(I_{CL}/100) - 1.44h^2 + 6.4h - 4.7 \quad (6)$$

Here R_c is the cutoff rigidity, h is the atmospheric pressure in mbar, N_{CL} is the mean hourly count of Climax NM, being approximately 400,000/h.

Coupling function (5) is dimensionless function, normalized to 1. It represents the distribution by the rigidities of primary particles in NM count, i.e. $W(R)dR$ is proportional to the flux of primaries in the rigidity range $R \dots R + dR$, which have contributed to observed value of NM count.

Coupling function for Tsumeb NM is shown in Fig. 4. It is derived from (5) by using the atmospheric pressure of Tsumeb location $h = 0.88$ mbar and $a \sim 10.7$, $k \sim 0.99$.

The asymptotic direction of Tsumeb NM can be derived by using PLANETOCOSMICS code [20], which provides asymptotic longitude and latitude versus rigidities. Asymptotic latitude changes little with rigidity, so we analyze only asymptotic longitude. Extracting Tsumeb longitude 17°E from asymptotic longitude, we obtain the angle A between asymptotic longitude and the zenith, which is used later on. The angle A is the function of rigidity: the larger is

R the smaller is A (see Fig. 4). Thus we have functions $W(R)$ and $A(R)$ for Tsumeb NM and based on those we derive function $D(A)$, which

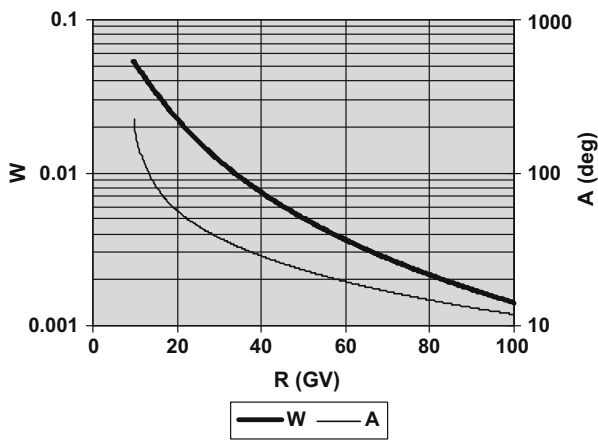


Fig. 4. Coupling function $W(R)$ and the angle $A(R)$ between the asymptotic and zenith longitudes versus the rigidity of Tsumeb location.

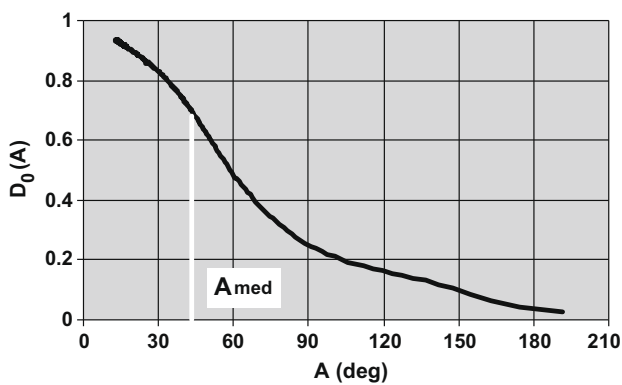


Fig. 5. Normalized directional function $D_0(A)$ of Tsumeb NM.

gives the distribution of primaries (flux) in NM count versus the angle A . We call $D(A)$ a “directional function” of NM. To do this note that $W(R)dR = W(R(A))(dR/dA)dA$, therefore the searched directional function $D(A)$ is

$$D(A) = W(R(A)) \left(\frac{dA}{dR} \right)^{-1} \quad (7)$$

Numerically calculating dA/dR from $A(R)$ and substituting it in (7) we derive directional function $D(A)$. Then dividing it on $D(0)$, we obtain the normalized directional function $D_0(A) = D(A)/D(0)$, shown in Fig. 5. Median value of A , calculated from $D_0(A)$ is $A_{med} \sim 43^\circ$ and the corresponding median rigidity is $R_{med} \sim 26$ GV. Thus the value A_{med} should be used only for determining averaged asymptotic longitude of the total flux. It implies that asymptotic direction of particles falling normally on Tsumeb location at e.g. LST = 8 h has RA = 8 h + $43^\circ/15^\circ/h \sim 11$ h, and not RA = 8 h (see Fig. 6). Thus we obtain sidereal variations versus RA of asymptotic directions, shown in Fig. 7. To derive the amplitude of error bars, note that mean hourly count of Tsumeb NM is about 11,000. During one year we sum 365 hourly records to obtain sidereal variations, and then use the data for 24 years (1977–2000). Therefore total count of sidereal variations,

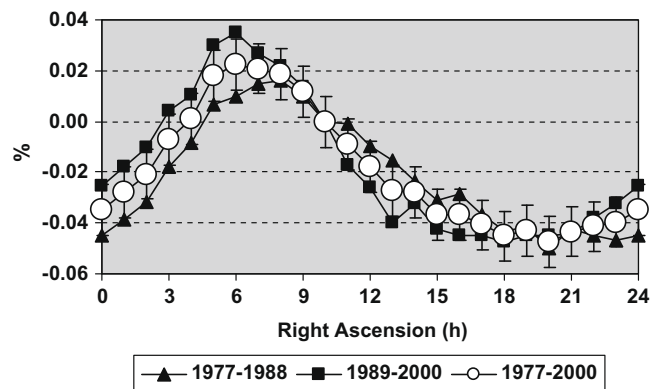


Fig. 7. Sidereal variations versus the right ascension of asymptotic direction. Error bars have the amplitude ± 0.01 .

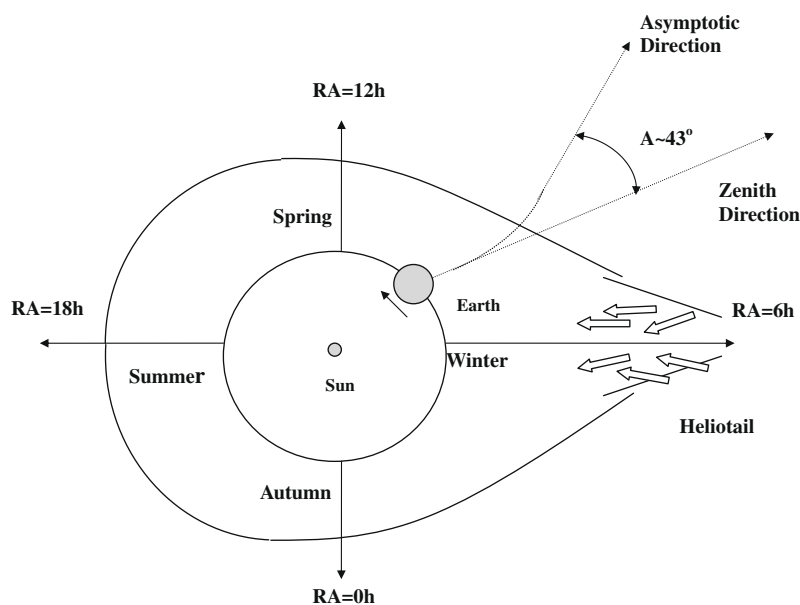


Fig. 6. Sketch of heliosphere, asymptotic and zenith directions in arbitrary scale. White arrows show additional flux of particles, coming from the direction of heliotail. View from above the ecliptic plane.

which in percentage is presented in Fig. 7 is about $11,000 \cdot 365 \cdot 24 = 96,360,000$. Its deviation (assuming that it is a Poissonian variable) is $100/96,360,000^{1/2} \sim 0.01\%$. Thus the amplitude of error bars corresponding to \pm one sigma is ± 0.01 .

4. Discussions and conclusion

Thus sidereal variations of Tsumeb NM count exhibits the maximal flux from asymptotic direction around $RA = 6$ h. This result coincides with the earlier derived results for high energy particles, where such anisotropy was called tail-in anisotropy because of its connection to heliotail. It is believed that the additional flux of particles flows into heliosphere due to interaction between the galactic and solar magnetic fields. It should be also noted that such an excess flux from heliotail can be conditioned as well by magnetic field configuration, tending to longitudinal shape around heliotail.

We have chosen two time intervals when magnetic field of the sun had opposite orientations: negative polarity state in the period 1977–1988 (when the sun's magnetic field at the sun's South Pole directs along the zenith) and positive polarity state in the period 1989–2000. According to [17], the reversal of the sun's magnetic field impacts the anisotropy, which has galactic origin, in a way that sidereal variations in negative polarity state are larger than those in positive state. However, in the data presented, the amplitude of anisotropy in negative state is not larger than that of positive state (0.07% and 0.08%, respectively, see Fig. 7). This means that the origin of anisotropy found is "heliospheric" and not "galactic".

Let us investigate the anisotropy amplitude separately in two semi-year periods: summer solstice, including April–September and winter solstice including October–March. In [12,14] the authors report larger anisotropy amplitude in winter solstice, explaining it by the closeness of the Earth to the heliotail in winter. To check this result for our case, in the data analysis above the number of days 365 should be changed to 182. The resulting seasonal sidereal variations are presented in Fig. 8. Unlike to 1-year periods of Fig. 7, here the error bars' amplitude is ± 0.014 . Although the amplitude of anisotropy in winter solstice (0.04%) is slightly larger than that in summer solstice (0.03%), nevertheless we can not neglect the possible random nature of such surplus, taking into account the error bars. Therefore the relationships between the amplitudes of anisotropy in winter and summer solstices for our case of ~ 25 GeV particles, remains unclear.

In conclusion we investigated sidereal variations of CR with median energy ~ 25 GeV by using Tsumeb NM data during 1977–2000. An excess flux was found with the amplitude $\sim 0.07\%$ at $LST \sim 3$ h, which corresponds to asymptotic direction of $RA \sim 6$ h. This excess flux is not decreased with the reversal of sun's magnetic field from negative polarity state in 1977–1988 to positive state in 1989–2000. Based on these features we conclude that

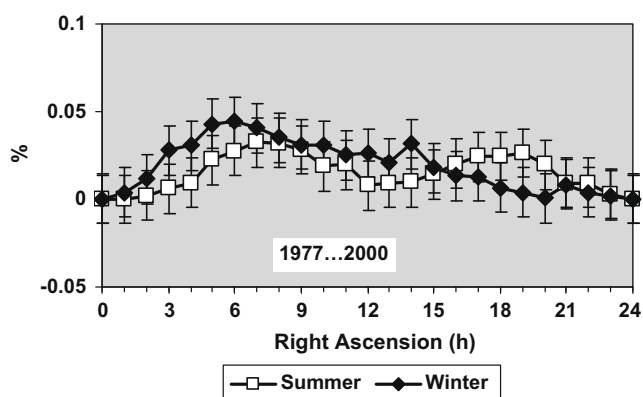


Fig. 8. Sidereal variations in summer (April–September) and winter (October–March) solstices. Error bars have the amplitude ± 0.014 .

our observed anisotropy is a *tail-in anisotropy* of low energy particles.

Acknowledgements

I thank N.Kh. Bostanjyan, A.A. Chilingarian, H.S. Martirosyan for discussions; T.G. Karapetyan for editing the manuscript, as well as P. Stoker for using Tsumeb NM's data. This work was supported by ISTC Grant A 1554.

References

- [1] A.G. Fenton, R.M. Jacklyn, R.B. Taylor, II. Nuovo Cimento. 22 (1961) 3985–3996.
- [2] R.M. Jacklyn, Nature 211 (1966) 690–693.
- [3] K. Nagashima, S. Mori, in: Proceedings of the ICRC on High Energy CR Modulation, Tokyo University, Japan, 1976, pp. 326–360.
- [4] P. Kiraly, J. Kota, J.L. Osborne, et al., Riv. Nuovo Cimento. 2 (1979) 1–46.
- [5] K. Munakata et al., Kamiokande Collaboration, Phys. Rev. D56 (1997) 23–26.
- [6] D.L. Hall, K. Munakata, S. Yasue, et al., J. Geophys. Res. 104 (1999) 6737–6749.
- [7] T. Antoni et al., Astroph. J. 604 (2004) 687–692.
- [8] G. Gaillian, Proceedings 29 ICRC (2005) 101–104.
- [9] M. Amenomori et al., The Tibet AS Collaboration, Astroph. J. 626 (2005) L29–L32.
- [10] M. Amenomori et al., Science 314 (2006) 439–443.
- [11] K. Nagashima, K. Fujimoto, R.M. Jacklyn, Proceedings 24 ICRC (1996) 652–655.
- [12] K. Nagashima, K. Fujimoto, R.M. Jacklyn, J. Geophys. Res. 103 (1998) 17429–17440.
- [13] A.H. Compton, I.A. Getting, Phys. Rev. 47 (1935) 817–821.
- [14] K. Fujimoto, H. Kojima, Z. Fujii, et al., Proceedings 27 ICRC (2001) 3927–3930.
- [15] K. Nagashima, Z. Fujii, Earth Planets Space 58 (2006) 1487–1498.
- [16] K. Nagashima, Y. Ishida, S. Mori, I. Morishita, Planet Space Sci. 31 (1983) 1269–1278.
- [17] K. Nagashima, I. Kondo, Z. Fujii, Earth Planets Space 57 (2005) 1083–1091.
- [18] H. Kojima, S.K. Gupta, Y. Hayashi, et al., Proceedings 29 ICRC (2005) 81–84.
- [19] L.I. Dorman, Cosmic Rays in the Earth's Atmosphere and Underground, Kluwer Academic Publishers, 2004.
- [20] <<http://cosray.unibe.ch/~laurent/planetocosmics/>>.